

Structural and Co-conformational Effects of Alkyne-Derived Subunits in Charged Donor–Acceptor [2]Catenanes

Ognjen Š. Miljanić,[†] William R. Dichtel,^{†,‡} Saeed I. Khan,[†] Shahab Mortezaei,[†] James R. Heath,[‡] and J. Fraser Stoddart^{*,†}

Contribution from California NanoSystems Institute and Department of Chemistry and Biochemistry, University of California, Los Angeles, 405 Hilgard Avenue, Los Angeles, California 90095, and Division of Chemistry and Chemical Engineering, California Institute of Technology, 1200 East California Boulevard, Pasadena, California 91125

Received February 24, 2007; E-mail: stoddart@chem.ucla.edu

Abstract: Four donor–acceptor [2]catenanes with cyclobis(paraquat-*p*-phenylene) (CBPQT⁴⁺) as the π -electron-accepting cyclophane and 1,5-dioxynaphthalene (DNP)-containing macrocyclic polyethers as π -electron donor rings have been synthesized under mild conditions, employing Cu⁺-catalyzed Huisgen 1,3-dipolar cycloaddition and Cu²⁺-mediated Eglinton coupling in the final steps of their syntheses. Oligoether chains carrying terminal alkynes or azides were used as the key structural features in template-directed cyclizations of [2]pseudorotaxanes to give the [2]catenanes. Both reactions proceed well with precursors of appropriate oligoether chain lengths but fail when there are only three oxygen atoms in the oligoether chains between the DNP units and the reactive functional groups. The solid-state structures of the donor–acceptor [2]catenanes confirm their mechanically interlocked nature, stabilized by $[\pi \cdots \pi]$, $[C-H \cdots \pi]$, and $[C-H \cdots O]$ interactions, and point to secondary noncovalent contacts between 1,3-butadiyne and 1,2,3-triazole subunits and one of the bipyridinium units of the CBPQT⁴⁺ ring. These contacts are characterized by the roughly parallel orientation of the inner bipyridinium ring system and the 1,2,3-triazole and 1,3-butadiyne units, as well as by the short $[\pi \cdots \pi]$ distances of 3.50 and 3.60 Å, respectively. Variable-temperature ¹H NMR spectroscopy has been used to identify and quantify the barriers to the conformationally and co-conformationally dynamic processes. The former include the rotations of the phenylene and the bipyridinium ring systems around their substituent axes, whereas the latter are confined to the circumrotation of the CBPQT⁴⁺ ring around the DNP binding site. The barriers for the three processes were found to be successively 14.4, 14.5–17.5, and 13.1–15.8 kcal mol^{−1}. Within the limitations of the small dataset investigated, emergent trends in the barrier heights can be recognized: the values decrease with the increasing size of the π -electron-donating macrocycle and tend to be lower in the sterically less encumbered series of [2]catenanes containing the 1,3-butadiyne moiety.

Introduction

Catenanes, topologically nontrivial molecules possessing two or more mechanically interlocked rings, have been known¹ for nearly half a century. The current renaissance in their chemistry, brought about by the judicious use of molecular recognition² and self-assembly³ aiding and abetting their template-directed synthesis,⁴ has elevated them from exotic (but little used) synthetic targets to potentially broadly applicable chemical compounds in the context of artificial molecular machines⁵ and molecular electronic devices.⁶ Bi- and multistable [2]catenanes have been used to effect unidirectional molecular motion^{5e,f,7}

and reversible molecular switching.^{6a,d,i,8} Recently, tristable donor–acceptor [2]catenanes have been proposed⁹ as the color-changing elements of electronic paper and displays.

We have a long-standing interest in the template-directed⁴ synthesis and the potential applications^{8,9} of charged donor–acceptor catenanes, based on cyclobis(paraquat-*p*-phenylene)¹⁰ (CBPQT⁴⁺ in Figure 1) as the π -electron acceptor. Although a

[†] University of California.

[‡] California Institute of Technology.

(1) Wasserman, E. *J. Am. Chem. Soc.* **1960**, *82*, 4433–4434.

(2) (a) Lehn, J.-M. *Supramolecular Chemistry*; VCH: Weinheim, 1999. (b) Schneider, H.-J.; Yatsimirsky, A. *Principles and Methods in Supramolecular Chemistry*; Wiley-VCH: Weinheim, 2000. (c) Steed, J. W.; Atwood, J. L. *Supramolecular Chemistry*; Wiley-VCH: Weinheim, 2000. (d) Lindoy, L. F.; Atkinson, I. M. In *Self-Assembly in Supramolecular Systems*; Stoddart, J. F., Ed.; Royal Society of Chemistry: Cambridge, 2000. (e) Lehn, J.-M. *Science* **2002**, *295*, 2400–2403. (f) Reinholdt, D. N.; Crego-Calama, M. *Science* **2002**, *295*, 2403–2407.

(3) (a) Lindsey, J. S. *New J. Chem.* **1991**, *15*, 153–180. (b) Philp, D.; Stoddart, J. F. *Synlett* **1991**, 445–458. (c) Lawrence, D. S.; Jiang, T.; Levitt, M. *Chem. Rev.* **1995**, *95*, 2229–2260. (d) Philp, D.; Stoddart, J. F. *Angew. Chem., Int. Ed. Engl.* **1996**, *35*, 1154–1156. (e) Stang, P. J.; Olenyuk, B. *Acc. Chem. Res.* **1997**, *30*, 502–518. (f) Conn, M. M.; Rebek, J., Jr. *Chem. Rev.* **1997**, *97*, 1647–1668. (g) Linton, B.; Hamilton, A. D. *Chem. Rev.* **1997**, *97*, 1669–1680. (h) Fujita, M. *Chem. Soc. Rev.* **1998**, *27*, 417–425. (i) Bong, D. T.; Clark, T. D.; Granja, J. R.; Ghadiri, M. R. *Angew. Chem., Int. Ed.* **2001**, *40*, 988–1011. (j) Prins, L. J.; Reinholdt, D. N.; Timmerman, P. *Angew. Chem., Int. Ed.* **2001**, *40*, 2382–2426. (k) Grieg, L. M.; Philp, D. *Chem. Soc. Rev.* **2001**, *30*, 287–302. (l) *Science* **2002**, *295*, 2400–2421 (Viewpoint on Supramolecular Chemistry and Self-Assembly). (m) Collin, J.-P.; Heitz, V.; Sauvage, J.-P. *Top. Curr. Chem.* **2005**, *262*, 29–62. (n) Schalley, C. A.; Weilandt, T.; Brüggemann, J.; Vögtle, F. *Top. Curr. Chem.* **2004**, *248*, 141–200. (o) Sauvage, J.-P.; Dietrich-Buchecker, C., Eds. *Molecular Catenanes, Rotaxanes and Knots*; Wiley-VCH: Weinheim, 1999. (p) Amabilino, D. B.; Stoddart, J. F. *Chem. Rev.* **1995**, *95*, 2725–2828.

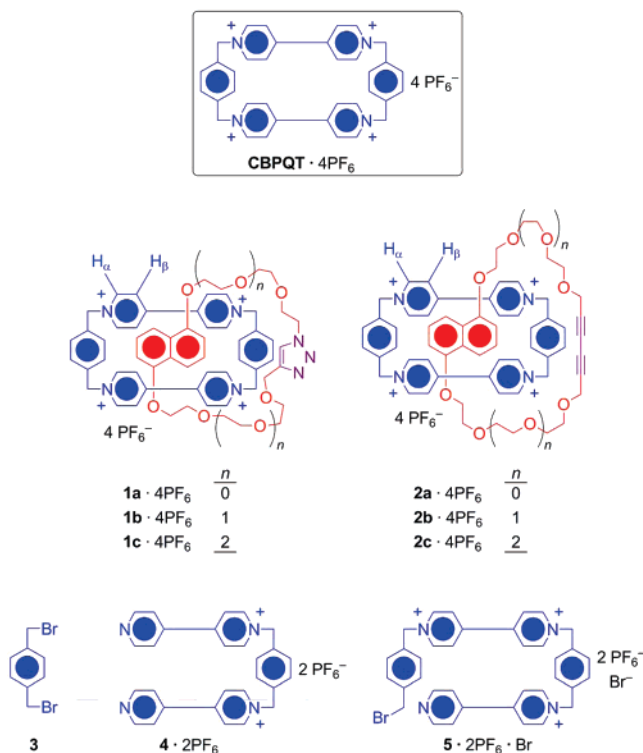


Figure 1. Cyclobis(paraquat-*p*-phenylene) (CBPQT⁴⁺), the catenanes **1a**–**c**·4PF₆ and **2a**–**c**·4PF₆, and the precursors (**3**, **4**·2PF₆, and **5**·2PF₆·Br) to CBPQT·4PF₆.

number of interesting π -donors¹¹ has been demonstrated to bind to CBPQT⁴⁺, in the past catenanes have been constructed primarily with hydroquinone,¹² resorcinol,¹³ dihydroxynaphthalene (DNP),¹⁴ and tetrathiafulvalene derivatives¹⁵ as electron-rich binding sites. Two ways (Figure 2) of synthesizing donor–acceptor [2]catenanes can be envisioned conceptually. Assuming the donor–acceptor interaction as a prerequisite, the catenation could proceed through either (i) threading of the acceptor component through the preformed donor ring, followed by the

cyclization of the acceptor or (ii) threading of the donor through the preformed acceptor ring and its subsequent cyclization (Figure 2a, b). A third approach, that of tandem heterocatenation (Figure 2c), can be proposed—and has indeed been realized in both neutral and charged donor–acceptor catenanes¹⁶—in which the formation of the donor and the acceptor rings happen concurrently. While undoubtedly elegant, tandem heterocatenation remains underutilized synthetically (because of its disappointing yields thus far) and is relatively unexplored mecha-

- (4) (a) Busch, D. H.; Stephenson, N. A. *Coord. Chem. Rev.* **1999**, *100*, 139–154. (b) Anderson, S.; Sanders, J. K. M. *Acc. Chem. Res.* **1993**, *26*, 469–475. (c) Cacciapaglia, R.; Mandolini, L. *Chem. Soc. Rev.* **1993**, *22*, 221–231. (d) Hoss, R.; Vögtle, F. *Angew. Chem., Int. Ed. Engl.* **1994**, *33*, 374–384. (e) Schneider, J. P.; Kelly, J. W. *Chem. Rev.* **1995**, *95*, 2169–2187. (f) Raymo, F. M.; Stoddart, J. F. *Pure Appl. Chem.* **1996**, *68*, 313–322. (g) Diederich, F.; Stang, P. J., Eds. *Templated Organic Synthesis*; Wiley-VCH: Weinheim, 1999. (h) Stoddart, J. F.; Tseng, H.-R. *Proc. Natl. Acad. Sci. U.S.A.* **2002**, *99*, 4797–4800. (i) Aricó, F.; Badjić, J. D.; Cantrill, S. J.; Flood, A. H.; Leung, K. C.-F.; Liu, Y.; Stoddart, J. F. *Top. Curr. Chem.* **2005**, *249*, 203–259. (j) Williams, A. R.; Northrop, B. H.; Chang, T.; Stoddart, J. F.; White, A. J. P.; Williams, D. J. *Angew. Chem., Int. Ed.* **2006**, *45*, 6665–6669. (k) Northrop, B. H.; Aricó, F.; Tangchiavang, N.; Badjić, J. D.; Stoddart, J. F. *Org. Lett.* **2006**, *8*, 3899–3902. (l) Cantrill, S. J.; Poulin-Kerstein, K. G.; Grubbs, R. H.; Lanari, D.; Leung, K. C.-F.; Nelson, A.; Smidt, S. P.; Stoddart, J. F.; Tirrell, D. A. *Org. Lett.* **2005**, *7*, 4213–4216.
- (5) (a) Balzani, V.; Credi, A.; Raymo, F. M.; Stoddart, J. F. *Angew. Chem., Int. Ed.* **2000**, *39*, 3348–3391. (b) Balzani, V.; Credi, A.; Venturi, M. *Molecular Devices and Machines: A Journey into the Nano World*; Wiley-VCH: Weinheim, 2003. (c) Huang, T. J.; Brough, B.; Ho, C.-M.; Liu, Y.; Flood, A. H.; Bonvallet, P. A.; Tseng, H.-R.; Stoddart, J. F.; Baller, M.; Magonov, S. *Appl. Phys. Lett.* **2004**, *85*, 5391–5393. (d) Liu, Y.; Flood, A. H.; Bonvallet, P. A.; Vignon, S. A.; Tseng, H.-R.; Huang, T. J.; Brough, B.; Baller, M.; Magonov, S.; Solares, S.; Goddard, W. A., III; Ho, C.-M.; Stoddart, J. F. *J. Am. Chem. Soc.* **2005**, *127*, 9745–9759. (e) Kay, E. R.; Leigh, D. A. *Top. Curr. Chem.* **2005**, *262*, 133–177. (f) Braunschweig, A. B.; Northrop, B. H.; Stoddart, J. F. *J. Mater. Chem.* **2006**, *16*, 32–44. (g) Browne, W. R.; Feringa, B. L. *Nat. Nanotechnol.* **2006**, *1*, 25–35. (h) Kay, E. R.; Leigh, D. A.; Zerbetto, F. *Angew. Chem., Int. Ed.* **2007**, *46*, 71–191. (i) Serrelli, V.; Lee, C.-F.; Kay, E. R.; Leigh, D. A. *Nature* **2007**, *445*, 523–527. (j) Saha, S.; Stoddart, J. F. *Chem. Soc. Rev.* **2007**, *77*–92.
- (6) (a) Luo, Y.; Collier, C. P.; Jeppesen, J. O.; Nielsen, K. A.; DeIonno, E.; Ho, G.; Perkins, J.; Tseng, H.-R.; Yamamoto, T.; Stoddart, J. F.; Heath, J. R. *ChemPhysChem* **2002**, *3*, 519–525. (b) Tseng, H.-R.; Nu, D.; Fang, N. X.; Zhang, X.; Stoddart, J. F. *ChemPhysChem* **2004**, *5*, 111–116. (c) Flood, A. H.; Ramirez, R. J.; Deng, W.-Q.; Miller, R. P.; Goddard, W. A., III; Stoddart, J. F. *Aust. J. Chem.* **2004**, *57*, 301–322. (d) Flood, A. H.; Stoddart, J. F.; Steuerman, D. W.; Heath, J. R. *Science* **2004**, *306*, 2055–2056. (e) Mendes, P. M.; Flood, A. H.; Stoddart, J. F. *Appl. Phys. A* **2005**, *80*, 1197–1209. (f) Moonen, N. N. P.; Flood, A. H.; Fernandez, J. M.; Stoddart, J. F. *Top. Curr. Chem.* **2005**, *262*, 99–132. (g) Beckman, R.; Beverly, K.; Boukai, A.; Bunimovich, Y.; Choi, J. W.; DeIonno, E.; Green, J.; Johnston-Halperin, E.; Luo, Y.; Sheriff, B.; Stoddart, J. F.; Heath, J. R. *Faraday Discuss.* **2006**, *131*, 9–22. (h) DeIonno, E.; Tseng, H.-R.; Harvey, D. D.; Stoddart, J. F.; Heath, J. R. *J. Phys. Chem. B* **2006**, *110*, 7609–7612. (i) Flood, A. H.; Wong, E. W.; Stoddart, J. F. *Chem. Phys.* **2006**, *324*, 280–290. (j) Green, J. E. et al. *Nature* **2007**, *445*, 414–417. (k) Ball, P. *Nature* **2007**, *445*, 362–363. (l) Dichtel, W. R.; Heath, J. R.; Stoddart, J. F. *Phil. Trans. R. Soc. London Ser. A* **2007**, *365*, 1605–1625.
- (7) (a) Balzani, V.; Credi, A.; Ferrer, B.; Silvi, S.; Venturi, M. *Top. Curr. Chem.* **2005**, *262*, 1–27. (b) Mandl, C. P.; König, B. *Angew. Chem., Int. Ed.* **2004**, *43*, 1622–1624. (c) Hernández, J. V.; Kay, E. R.; Leigh, D. A. *Science* **2004**, *306*, 1532–1537. (d) Leigh, D. A.; Wong, J. K. Y.; Dehez, F.; Zerbetto, F. *Nature* **2003**, *424*, 174–179.
- (8) (a) Kim, Y.-H.; Jang, S. S.; Goddard, W. A. *Appl. Phys. Lett.* **2006**, *88*, 163112/1–163112/3. (b) Feringa, B. L., Ed. *Molecular Switches*; Wiley-VCH: Weinheim, 2001. (c) Alvaro, M.; Chretien, M. N.; Ferrer, B.; Fornes, V.; Garcia, H.; Scaiano, J. C. *Chem. Commun.* **2001**, *20*, 2106–2107. (d) Collier, C. P.; Mattersteig, G.; Wong, E. W.; Luo, Y.; Beverly, K.; Sampaio, J.; Raymo, F. M.; Stoddart, J. F.; Heath, J. R. *Science* **2000**, *289*, 1172–1175. (e) Choi, J. W.; Flood, A. H.; Steuerman, D. W.; Nygaard, S.; Braunschweig, A. B.; Moonen, N. N. P.; Laursen, B. W.; Luo, Y.; DeIonno, E.; Peters, A. J.; Jeppesen, J. O.; Xe, K.; Stoddart, J. F.; Heath, J. R. *Chem. Eur. J.* **2006**, *12*, 261–279.
- (9) (a) Ikeda, T.; Saha, S.; Aprahamian, I.; Leung, K. C.-F.; Williams, A.; Deng, W.-Q.; Flood, A. H.; Goddard, W. A.; Stoddart, J. F. *Chem.-Asian J.* **2007**, *2*, 76–93. (b) Deng, W.-Q.; Flood, A. H.; Stoddart, J. F.; Goddard, W. A. *J. Am. Chem. Soc.* **2005**, *127*, 15994–15995.
- (10) (a) Dodd, G.; Ercolani, G.; Mencarelli, P.; Piermattei, A. *J. Org. Chem.* **2005**, *70*, 3761–3764. (b) Asakawa, M.; Dehaen, W.; L'abbé, G.; Menzer, S.; Nouwen, J.; Raymo, F. M.; Stoddart, J. F.; Williams, D. J. *J. Org. Chem.* **1996**, *61*, 9591–9595. (c) Odell, B.; Reddington, M. V.; Slawin, A. M. Z.; Spencer, N.; Stoddart, J. F.; Williams, D. J. *Angew. Chem., Int. Ed. Engl.* **1988**, *27*, 1547–1550.
- (11) For indole derivatives, see: (a) Ashton, P. R.; Bissell, R. A.; Górski, R.; Philp, D.; Spencer, N.; Tolley, M. S. *Synlett* **1992**, 919–922. (b) Mirzorian, A.; Kaifer, A. E. *J. Org. Chem.* **1995**, *60*, 8093–8095. (c) Anelli, P.-L. et al. *Chem.-Eur. J.* **1997**, *3*, 1113–1135. For electron-rich biphenyls, see: (d) Córdova, E.; Bissell, R. A.; Spencer, N.; Ashton, P. R.; Stoddart, J. F.; Kaifer, A. E. *J. Org. Chem.* **1993**, *58*, 6550–6552. For neurotransmitters (dopamine, epinephrine, norepinephrine, and serotonin), see: (e) Bernardo, A. R.; Stoddart, J. F.; Kaifer, A. E. *J. Am. Chem. Soc.* **1992**, *114*, 10624–10631.
- (12) See, inter alia: (a) Ashton, P. R.; Goodnow, T. T.; Kaifer, A. E.; Reddington, M. V.; Slawin, A. M. Z.; Spencer, N.; Stoddart, J. F.; Vicent, C.; Williams, D. J. *Angew. Chem., Int. Ed. Engl.* **1989**, *28*, 1396–1399. (b) Brown, C. L.; Philp, D.; Stoddart, J. F. *Synlett* **1991**, 459–461. (c) Anelli, P.-L. et al. *J. Am. Chem. Soc.* **1992**, *114*, 193–218.
- (13) Amabilino, D. B.; Ashton, P. R.; Stoddart, J. F. *Supramolecular Chem.* **1995**, *5*, 5–8.
- (14) See, inter alia: Ashton, P. R. et al. *J. Chem. Soc., Chem. Commun.* **1991**, 634–639.
- (15) See, inter alia: (a) Ballardini, R.; Balzani, V.; Di Fabio, A.; Gandolfi, M. T.; Becher, J.; Lau, J.; Nielsen, M. B.; Stoddart, J. F. *New J. Chem.* **2001**, *25*, 293–298. (b) Li, Z.-T.; Stein, P. C.; Becher, J.; Jensen, D.; Moerk, P.; Svenstrup, N. *Chem.-Eur. J.* **1996**, *2*, 624–633. (c) Asakawa, M. et al. *Angew. Chem., Int. Ed.* **1998**, *37*, 333–337.
- (16) (a) Hamilton, D. G.; Prodi, L.; Feeder, N.; Sanders, J. K. M. *J. Chem. Soc., Perkin Trans. 1* **1999**, 1057–1065. (b) Hamilton, D. G.; Feeder, N.; Prodi, L.; Teat, S. J.; Clegg, W.; Sanders, J. K. M. *J. Am. Chem. Soc.* **1998**, *120*, 1096–1097. (c) Miljanić, O. S.; Dichtel, W. R.; Mortezaei, S.; Stoddart, J. F. *Org. Lett.* **2006**, *8*, 4835–4838. For early examples of a related synthetic approach, *homocatenation*, in which the [2]catenane rings are identical, see: (d) Johnston, A. G.; Leigh, D. A.; Pritchard, R. J.; Deegan, M. D. *Angew. Chem., Int. Ed. Engl.* **1995**, *34*, 1209–1212. (e) Vögtle, F.; Meier, S.; Hoss, R. *Angew. Chem., Int. Ed. Engl.* **1992**, *31*, 1619–1622. (f) Hunter, C. A. *J. Am. Chem. Soc.* **1992**, *114*, 5303–5311. (g) Dietrich-Buchecker, C. O.; Sauvage, J.-P.; Kintzinger, J. P. *Tetrahedron Lett.* **1983**, *24*, 5095–5098.

nistically. Since it has not been strictly proven that both rings form *simultaneously* during the course of this reaction, it is possible that tandem heterocatenation still proceeds via a cyclization–templation–catenation cascade, but with the difference that either the donor or the acceptor can take on the role of the template with the outcome being identical.

In our previous syntheses of CBPQT⁴⁺-based [2]catenanes, the donor ring components were used exclusively as templates. Typically, 1,4-bis(bromomethyl)benzene (**3** in Figure 1) and 1,1'-[1,4-phenylene bis(methylene)]-bis-4,4'-bipyridinium hexafluorophosphate (**4**·2PF₆ in Figure 1) cyclize to become a CBPQT⁴⁺ ring, encircled around a suitable macrocyclic donor template (Figure 2d,e). The intermediacy of a [2]pseudorotaxane that is formed from the donor macrocycle and the partially cyclized tricationic acceptor thread (**5**·2PF₆·Br in Figure 1) has been confirmed experimentally,¹⁷ although this species is normally not isolated. The alternative route, wherein the acceptor ring templates the cyclization of the donor macrocycle, has not yet been explored to our knowledge. The reason is probably the chemical sensitivity of CBPQT⁴⁺·4PF₆. Its stability has limited significantly the synthetic arsenal available for the closure of the donor macrocycle around the CBPQT⁴⁺ ring to give a donor–acceptor [2]catenane.

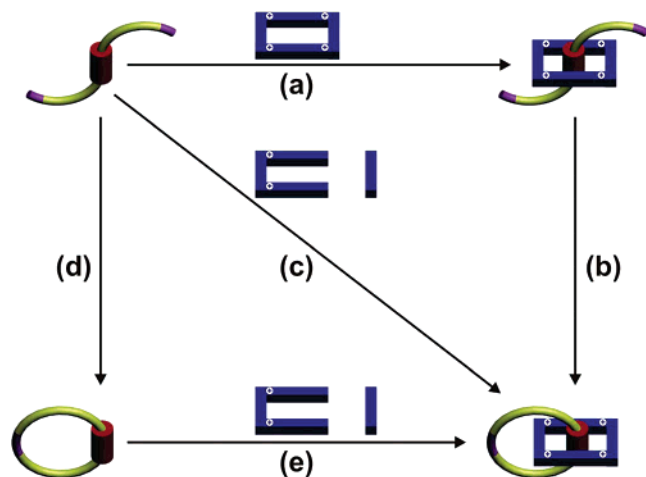


Figure 2. Alternative strategies in the template-directed synthesis of charged donor–acceptor [2]catenanes containing π -electron-rich crown ethers incorporating dioxybenzene and dioxynaphthalene units (red) and the π -electron-deficient tetracationic cyclophane, cyclobis(paraquat-*p*-phenylene) (CBPQT⁴⁺, blue). Alternative heterocatenation strategies are (i) threading (a) of the CBPQT⁴⁺ ring by an acyclic precursor of the crown ether, followed by clipping (b) to form the crown ether itself; (ii) all-in-one tandem heterocatenation approach (c), and (iii) macrocyclization (d) to give the crown ether, followed by clipping (e) to form the CBPQT⁴⁺ ring.

The constitution of CBPQT⁴⁺ points to the reaction conditions being a delicate balance between certain extremes. As a tetracation, the cyclophane is sensitive to reducing agents. The strain in the cyclophane facilitates nucleophilic attack at the benzylic positions, displacing the positively charged bipyridinium unit. Finally, basic conditions appear to be equally harmful, presumably (but not certainly) because deprotonation of the benzylic methylene group leads to a number of rearranged and ring-opened products.

While these disadvantages restrict the synthetic options, they certainly do not eliminate them entirely. Hence, reactions have been sought after that employ neutral (or mildly acidic), oxidative, and nucleophile-free conditions. Both the click reaction¹⁸ and Eglinton coupling¹⁹ were selected as promising candidates, since they proceed at roughly neutral pH,²⁰ are essentially nucleophile-free,²¹ and in the case of Eglinton coupling, proceed under oxidative conditions.

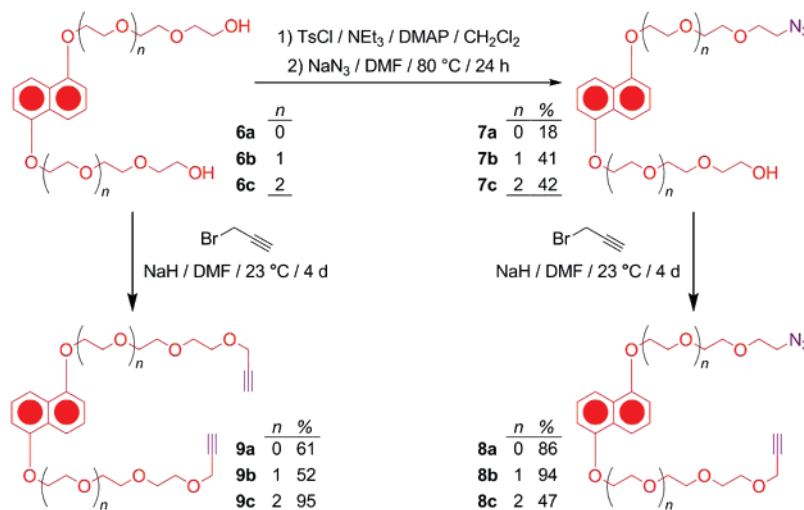
In a preliminary communication^{16c} we have demonstrated the feasibility of cyclizing [2]pseudorotaxanes based on the CBPQT⁴⁺ π -accepting ring and macrocyclic polyethers incorporating DNP as the π -donors into the [2]catenanes **1b**·4PF₆ and **2b**·4PF₆ (Figure 1) using the Cu⁺-catalyzed Huisgen 1,3-cycloaddition between an alkyne and an azide (“click” reaction) and the Cu²⁺-mediated Eglinton coupling, respectively. This paper presents an examination of the scope and limitations of the revised protocols for the synthesis of catenanes **1b,c**·4PF₆ and **2b,c**·4PF₆ and the attempted synthesis of [2]catenanes **1a**·4PF₆ and **2a**·4PF₆. An X-ray crystal structure of the envisioned [2]pseudorotaxane precursor to **2a**·4PF₆ reveals a possible reason for the failure of the template-directed synthesis⁴ in its case. Crystallographically characterized catenanes **1b**·4PF₆ and **2b,c**·4PF₆ parallel analogous DNP/CBPQT⁴⁺-based systems in their interlocked nature and the alignment of the donor and acceptor units but also indicate additional interactions between the 1,2,3-triazole (**1b**·4PF₆) and 1,3-butadiyne (**2b,c**·4PF₆) moieties and the inner bipyridinium unit of the CBPQT⁴⁺ ring. Finally, dynamic ¹H NMR spectroscopic investigations show the dependence of conformational and co-conformational freedom on the size and nature of the [2]catenanes and allow us to identify and quantify the barriers to several dynamic processes occurring in the new catenated compounds.

Syntheses

The synthetic objectives of the present investigation were, in part, inspired by the demonstrated²² viability of the synthesis of [2]rotaxanes of different types through the use of the Cu⁺-catalyzed Huisgen 1,3-dipolar cycloaddition²³ of azides and

(17) (a) D’Acerno, C.; Doddi, G.; Ercolani, G.; Mencarelli, P. *Chem.–Eur. J.* **2000**, *6*, 3540–3546. (b) Capobianchi, S.; Doddi, G.; Ercolani, G.; Mencarelli, P. *J. Org. Chem.* **1998**, *63*, 8088–8089. (c) Capobianchi, S.; Doddi, G.; Ercolani, G.; Keyes, J. W.; Mencarelli, P. *J. Org. Chem.* **1997**, *62*, 7015–7017. (d) Brown, C. L.; Philp, D.; Spencer, N.; Stoddart, J. F. *Isr. J. Chem.* **1992**, *32*, 61–67.

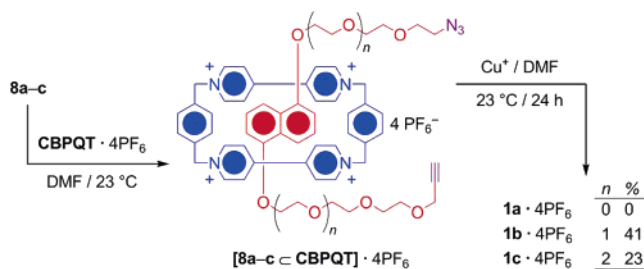
(18) (a) Rostovtsev, V. V.; Green, L. G.; Fokin, V. V.; Sharpless, K. B. *Angew. Chem., Int. Ed.* **2002**, *41*, 2596–2599. (b) Kolb, H. C.; Finn, M. G.; Sharpless, K. B. *Angew. Chem., Int. Ed.* **2001**, *40*, 2004–2021. (c) Tornøe, C. W.; Christensen, C.; Meldal, M. *J. Org. Chem.* **2002**, *67*, 3057–3064. (19) For a review of Glaser, Eglinton, and related alkyne couplings, see: (a) Siemsen, P.; Livingston, R. C.; Diederich, F. *Angew. Chem., Int. Ed.* **2000**, *39*, 2632–2657. For the original report, see: (b) Eglinton, G.; Galbraith, A. R. *Chem. Ind. (London)* **1956**, 737–738. (20) It is worth noting that the vast majority of reported Eglinton’s couplings uses basic amines as solvents. In our work, we adapted the following two protocols which report successful reactions in MeCN and DMF, respectively. See: (a) Meissner, U.; Meissner, B.; Staab, H. A. *Angew. Chem., Int. Ed. Engl.* **1973**, *12*, 916–918. (b) Berscheid, R.; Vögtle, F. *Synthesis*, **1992**, 58–62. (21) Typical reaction conditions for the click reaction involve CuSO₄·5H₂O/ascorbic acid as catalysts, while Eglinton coupling uses Cu(OAc)₂·H₂O. The SO₄²⁻ dianion is virtually nonnucleophilic, while the AcO⁻ anion has weak nucleophilic character which did not present a significant problem in our experiments. (22) (a) Dichtel, W. R.; Miljanić, O. Š.; Spruell, J. M.; Heath, J. R.; Stoddart, J. F. *J. Am. Chem. Soc.* **2006**, *128*, 10388–10390. (b) Aucagne, V.; Hänni, K. D.; Leigh, D. A.; Lusby, P. J.; Walker, D. B. *J. Am. Chem. Soc.* **2006**, *128*, 2186–2187. (c) Mobian, P.; Collin, J.-P.; Sauvage, J.-P. *Tetrahedron Lett.* **2006**, *47*, 4907–4909. (d) Aprahamian, I.; Dichtel, W. R.; Ikeda, T.; Heath, J. R.; Stoddart, J. F. *Org. Lett.* **2007**, *9*, 1287–1290. (e) Braunschweig, A. B.; Dichtel, W. R.; Miljanić, O. Š.; Olson, M. A.; Spruell, J. M.; Khan, S. I.; Heath, J. R.; Stoddart, J. F. *Chem. Asian J.* **2007**, *2*, 634–647. (23) (a) Huisgen, R. *Pure Appl. Chem.* **1989**, *61*, 613–628. (b) Huisgen, R.; Szeimies, G.; Möbius, L. *Chem. Ber.* **1967**, *100*, 2494–2507. (c) Lwowski, W. In *1,3-Dipolar Cycloaddition Chemistry*; Padwa, A., Ed.; Wiley: New York, 1984; Vol. 1, Chapter 5. (d) Bastide, J.; Hamelin, J.; Texier, F.; Ven, V. Q. *Bull. Chim. Soc. Fr.* **1973**, 2555–2579. (e) Bastide, J.; Hamelin, J.; Texier, F.; Ven, V. Q. *Bull. Chim. Soc. Fr.* **1973**, 2871–2887.

Scheme 1. Synthesis of Precursors to π -Donating Rings in Catenanes **1a–c**·4PF₆ and **2a–c**·4PF₆

alkynes (“click” reaction¹⁸) by our^{22a} and other^{22b,c} groups. The tolerance of complex formation under the conditions of the click reaction is noteworthy, and this mild reaction has found use in the construction of many diverse systems.^{18,24} More specifically, our work on DNP/CBPQT⁴⁺-based [2]pseudorotaxanes showed²² that these 1:1 complexes can be stoppered efficiently by click reactions between an azide-terminated DNP rod and alkyne-functionalized bulky stoppers. On a fundamental level, this result demonstrates that copper acetylides (as the proposed mechanistic intermediates in the click reaction²⁵) are compatible both with the [2]pseudorotaxane components—especially the sensitive CBPQT⁴⁺ ring—and the complexation which occurs between them. This realization readily translated into the challenge to synthesize [2]catenanes and prompted our investigations of the utility of the Eglinton oxidative alkyne homocoupling,¹⁹ another reaction proceeding through intermediate copper acetylides. The mechanistically related Glaser’s alkyne homocoupling has been employed previously²⁶ in the syntheses of [2]- and [3]catenanes

based on donor–acceptor (Sanders, Gunter),²⁷ transition metal–ligand (Sauvage),²⁸ and transient covalent bond (Godt)²⁹ templating strategies.

Preparation of suitable DNP-based precursors for the click reaction commences (Scheme 1) with 1,5-oligo(ethyleneglycol)-DNP derivatives **6a–c** as the starting materials.³⁰ These materials can be readily converted into the corresponding monotosylates³¹ which are then subjected to nucleophilic substitutions with sodium azide to produce the azides **7a–c**. Subsequent deprotonations of the free hydroxyl groups were followed by alkylation with propargyl bromide to yield the azidoalkynes **8a–c**. Exposure of **8a–c** to CBPQT·4PF₆ in either DMF or MeCN gave (Scheme 2) intensely purple-colored

Scheme 2

solutions, indicative of the formation of the pseudorotaxanes [8 ⊂ CBPQT]·4PF₆. Subjecting these [2]pseudorotaxanes to the classical click conditions (CuSO₄·5H₂O/ascorbic acid or CuI, in DMF or MeCN) gave the desired [2]catenanes **1b**·4PF₆ and

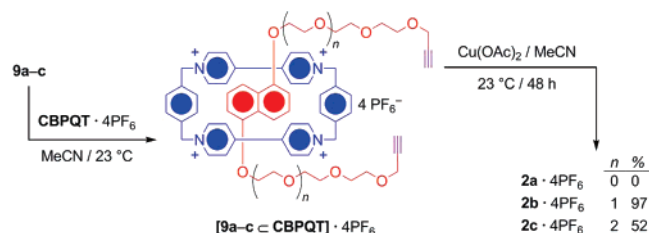
- (24) (a) Hawker, C. J.; Wooley, K. L. *Science* **2005**, *309*, 1200–1205. (b) Goodall, G. W.; Hayes, W. *Chem. Soc. Rev.* **2006**, *35*, 280–312. (c) Diaz, D. D.; Punna, S.; Holzer, P.; McPherson, A. K.; Sharpless, K. B.; Fokin, V. V.; Finn, M. G. *J. Polym. Sci., Part A: Polym. Chem.* **2004**, *42*, 4392–4403. (d) Laurent, B. A.; Grayson, S. M. *J. Am. Chem. Soc.* **2006**, *128*, 4238–4239. (e) Riva, R.; Schmeits, P.; Stoffelbach, F.; Jerome, C.; Jerome, R.; Lecomte, P. *Chem. Commun.* **2005**, 5334–5336. (f) Opsteen, J. A.; van Hest, J. C. M. *Chem. Commun.* **2005**, 57–59. (g) Lutz, J. F.; Börner, H. G.; Weichenhan, K. *Macromol. Rapid Commun.* **2005**, *26*, 514–518. (h) Ossipov, D. A.; Hilborn, J. *Macromolecules* **2006**, *39*, 2113–2120. (i) Wu, P.; Feldman, A. K.; Nugent, A. K.; Hawker, C. J.; Scheel, A.; Voit, B.; Pyun, J.; Fréchet, J. M. J.; Sharpless, K. B.; Fokin, V. V. *Angew. Chem., Int. Ed.* **2004**, *43*, 3928–3932. (j) Wu, P.; Malkoch, M.; Hunt, J. N.; Vestberg, R.; Kalitgrad, E.; Finn, M. G.; Fokin, V. V.; Sharpless, K. B.; Hawker, C. J. *Chem. Commun.* **2005**, 5775–5777. (k) Malkoch, M.; Schleicher, K.; Drockenmüller, E.; Hawker, C. J.; Russel, T. P.; Wu, P.; Fokin, V. V. *Macromolecules* **2005**, *38*, 3663–3678. (l) Lee, J. W.; Kim, B. K.; Kim, H. H.; Han, S. C.; Shin, W. S.; Hin, S. H. *Macromolecules* **2006**, *39*, 2418–2422. (m) Lee, J. W.; Kim, J. H.; Kim, B. K.; Shin, W. S.; Jin, S. H. *Tetrahedron* **2006**, *62*, 894–900. (n) Fernandez-Megia, E.; Correa, J.; Rodriguez-Meizoso, I.; Riguerera, R. *Macromolecules* **2006**, *39*, 2113–2120. (o) Helms, B.; Mynar, J. L.; Hawker, C. J.; Fréchet, J. M. J. *J. Am. Chem. Soc.* **2004**, *126*, 15020–15021. (p) Mynar, J. L.; Choi, T. L.; Yoshida, M.; Kim, V.; Hawker, C. J.; Fréchet, J. M. J. *Chem. Commun.* **2005**, 5169–5171. (q) Malcoch, M.; Thibault, R. J.; Drockenmüller, E.; Messerschmidt, M.; Voit, B.; Russel, T. P.; Hawker, C. J. *J. Am. Chem. Soc.* **2005**, *127*, 14942–14949.
- (25) (a) Bock, V. D.; Hiemstra, H.; van Maarseveen, J. H. *Eur. J. Org. Chem.* **2005**, *2006*, 51–68. (b) Himo, F.; Lovell, T.; Hilgraf, R.; Rostovtsev, V. V.; Noodleman, L.; Sharpless, K. B.; Fokin, V. V. *J. Am. Chem. Soc.* **2005**, *127*, 210–216. (c) Rodinov, V. O.; Fokin, V. V.; Finn, M. G. *Angew. Chem., Int. Ed.* **2005**, *44*, 2210–2215. (d) Nolte, C.; Mayer, P.; Straub, B. F. *Angew. Chem., Int. Ed.* **2007**, *46*, 2101–2103.
- (26) (a) Glaser, C. *Ber. Dtsch. Chem. Ges.* **1869**, *2*, 422–424. (b) Glaser, C. *Ann. Chem. Pharm.* **1870**, *154*, 137–171.

- (27) (a) Hamilton, D. G.; Sanders, J. K. M.; Davies, J. E.; Clégg, W.; Teat, S. J. *Chem. Commun.* **1997**, 897–898. (b) Gunter, M. J.; Farquhar, S. M. *Org. Biomol. Chem.* **2003**, *1*, 3450–3457.
- (28) (a) Dietrich-Buchecker, C. O.; Hemmert, C.; Khémis, A.-K.; Sauvage, J.-P. *J. Am. Chem. Soc.* **1990**, *112*, 8002–8008. (b) Dietrich-Buchecker, C. O.; Khémis, A.; Sauvage, J.-P. *J. Chem. Soc., Chem. Commun.* **1986**, 1376–1378.
- (29) (a) Godt, A. *Eur. J. Org. Chem.* **2004**, 1639–1645. (b) Duda, S.; Godt, A. *Eur. J. Org. Chem.* **2003**, 3412–3420. (c) Ünsal, Ö.; Godt, A. *Chem.–Eur. J.* **1999**, *5*, 1728–1733.
- (30) For **6a**, see: (a) Amabilino, D. B. et al. *J. Am. Chem. Soc.* **1995**, *117*, 11142–11170. For **6b** and **6c**, see: (b) Ashton, P. R.; Huff, J.; Menzer, S.; Parsons, I. W.; Preece, J. A.; Stoddart, J. F.; Tolley, M. S.; White, A. J. P.; Williams, D. J. *Chem.–Eur. J.* **1996**, *2*, 31–44.
- (31) The monotosylates of **6a** and **6b** have been reported previously. See, respectively: (a) Collier, C. P.; Jeppesen, J. O.; Liu, Y.; Perkins, J.; Wong, E. W.; Heath, J. R.; Stoddart, J. F. *J. Am. Chem. Soc.* **2001**, *123*, 12632–12641. (b) Liu, Y.; Saha, S.; Vignoni, S. A.; Flood, A. H.; Stoddart, J. F. *Synthesis* **2005**, *19*, 3437–3445.

$1c \cdot 4PF_6$ in 41% and 23% yields,^{16c} respectively, after purification by column chromatography. However, the [2]pseudorotaxane [**8a** \subset **CBPQT**] $\cdot 4PF_6$ failed to react, even after prolonged reaction times, and only unreacted **8a** and **CBPQT** $\cdot 4PF_6$ could be recovered, following the dethreading that undoubtedly occurs during chromatography.

Preparation of the precursors for the Eglinton coupling was significantly simpler as a consequence of the homocoupling nature of the reaction that utilizes symmetric starting materials. Thus, a one-step propargylation of **6a–c** (Scheme 1) gave **9a–c**, that is the compounds which can undergo the threading-followed-by-clipping cascade. Conversion of **9** to the corresponding [2]pseudorotaxanes [**9** \subset **CBPQT**] $\cdot 4PF_6$ was followed by exposure (Scheme 3) of the reaction mixture to 2 equiv of

Scheme 3



$Cu(OAc)_2 \cdot H_2O$ in MeCN. After 2 d at 23 °C, the [2]catenanes, **2b** $\cdot 4PF_6$ and **2c** $\cdot 4PF_6$, were isolated in 97% and 52% yields, respectively. The former result is a remarkable improvement over that in our original report^{16c} which utilized classical (23 °C, 5 d) and microwave-assisted³² (90 °C, 20 min) conditions to produce **2b** $\cdot 4PF_6$ in 14 and 21% yield, respectively. This outcome can be explained tentatively by a slow nucleophilic attack of the acetate counterion on the **CBPQT**⁴⁺ ring of the [2]catenane molecule, decreasing the yield of the catenation as it progresses past its optimal point. As in the earlier click series of reactions, the [2]pseudorotaxane [**9a** \subset **CBPQT**] $\cdot 4PF_6$ with the shortest precursor donor template failed to react, and only starting materials were recovered, albeit not completely, suggesting that partial polymerization might have occurred. The structural analysis of [**9a** \subset **CBPQT**] $\cdot 4PF_6$ reveals a possible explanation for this unfavorable synthetic outcome and, to some extent, for the failure of [**8a** \subset **CBPQT**] $\cdot 4PF_6$ to react. The X-ray crystal structure (for a detailed discussion of structural features vide infra) reveals that the $-C\equiv C-H$ units in [**9a** \subset **CBPQT**] $\cdot 4PF_6$ are pointing away from each other in the solid state (Figure 3) although this observation may be inconsequential for the solution-phase reactivity. However, in the hypothetical conformation of the threaded component in [**9a** \subset **CBPQT**] $\cdot 4PF_6$, in which one of the oligoether chains emanating from the DNP unit is reflected through the plane of the naphthalene ring thus bringing the two triple bonds close to each other, the alkyne hydrogen atoms are still separated by a very long 5.87 Å. The oligoether chains are simply too short to cyclize to give a polyether loop that would not be unreasonably strained.

Structural Investigations

The [2]catenanes **1b** $\cdot 4PF_6$, **2b** $\cdot 4PF_6$, and **2c** $\cdot 4PF_6$, as well as the pseudorotaxane [**9a** \subset **CBPQT**] $\cdot 4PF_6$, were all characterized

crystallographically. Single crystals of these compounds/complexes suitable for X-ray diffraction were grown by vapor diffusion of *i*-Pr₂O into solutions of the catenanes/pseudorotaxane in MeCN at 23 °C during 3–4 d. Crystal, unit cell, refinement, and some of the common structural parameters for the four crystal structures are listed in Table 1, and individual crystal structures/superstructures are shown in Figures 3–6. Despite extensive experimentation, no X-ray-quality crystals of **1c** $\cdot 4PF_6$ could be obtained.

The pseudorotaxane [**9a** \subset **CBPQT**] $\cdot 4PF_6$ crystallizes (Figure 3) without solvent incorporation, and the supermolecule has a crystallographic center of inversion. The interpenetrated superstructure is stabilized by (a) $[\pi \cdots \pi]$ stacking between the naphthalene ring of the DNP unit and the bipyridinium units of **CBPQT**⁴⁺ ring, (b) $[C-H \cdots \pi]$ interactions between the hydrogen atoms in the 4- and 8-positions of the DNP and the phenylene rings of the **CBPQT**⁴⁺ ring, and (c) $[C-H \cdots O]$ interactions (see Table 1 for corresponding distances) between the oxygen atoms in the side chain of **9a** and the bipyridinium α -hydrogen atoms in the **CBPQT**⁴⁺ ring.³³ Two symmetry-related PF_6^- ions are in close (2.40 Å) contact with the bipyridinium α -hydrogen atoms in the **CBPQT**⁴⁺ ring through the fluorine atoms. Unlike the DNP derivatives whose glycol chains were terminated with phenoxy groups,³⁴ the propargyl-terminated derivative **9a** forms only crystals of [**9a** \subset **CBPQT**] $\cdot 4PF_6$ on mixing with **CBPQT** $\cdot 4PF_6$, regardless of the ratio used (varied from 1:10 to 10:1) during the attempted crystallizations. The triple bonds of **9a** are positioned over the proximal pyridinium rings of the **CBPQT**⁴⁺ ring, rather than away from them. In the superstructure of [**9a** \subset **CBPQT**] $\cdot 4PF_6$, the closest intermolecular contacts are between the triple bonds of adjacent molecules, with distances between the centroids of the neighboring $C\equiv C$ bonds³⁵ alternating between 5.40 and 4.92 Å.

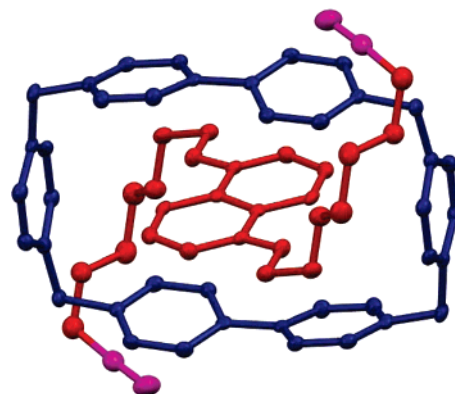


Figure 3. Solid-state superstructure of [**9a** \subset **CBPQT**]⁴⁺. Aside from the PF_6^- counterions, hydrogen atoms and solvent molecules are omitted for clarity. Thermal ellipsoids are shown at 50% probability levels. Acceptor ring is shown in blue, donor thread in red, and triple bonds in purple.

All three [2]catenanes crystallize in a $P\bar{1}$ space group, with a single pair of enantiomeric molecules³⁶ in the unit cell and

(32) For reviews of microwave-assisted reactions, see: (a) Kappe, O. C. *Angew. Chem., Int. Ed.* **2004**, *43*, 6250–6284. (b) Lindstrom, P.; Tierney, J.; Wathey, B.; Westman, J. *Tetrahedron Lett.* **2001**, *57*, 9225–9283.

(33) Asakawa, M. et al. *J. Org. Chem.* **1997**, *62*, 26–37.

(34) Depending on the ratio between the **CBPQT**⁴⁺ ring and the diphenoxy-terminated DNP polyether, crystals of 1:1 and 3:1 complexes could be isolated. See: Northrop, B. H.; Khan, S. I.; Stoddart, J. F. *Org. Lett.* **2006**, *8*, 2159–2162.

(35) These distances (as well as those in **2b** $\cdot 4PF_6$) are comparable to those observed in supramolecularly organized polymerizable diiodobutadiynes in the solid state: (a) Sun, A.; Lauher, J. W.; Goroff, N. S. *Science* **2006**, *312*, 1030–1034. (b) Goroff, N. S.; Curtis, S. M.; Webb, J. A.; Fowler, F. W.; Lauher, J. W. *Org. Lett.* **2005**, *7*, 1891–1893.

Table 1. Crystal, Unit Cell, Refinement, and Selected Structural Parameters of **[9a ⊂ CBPQT]·4PF₆**, **1b·4PF₆**, **2b·4PF₆**, and **2c·4PF₆**

cmpd	[9a ⊂ CBPQT]·4PF₆	1b·4PF₆	2b·4PF₆	2c·4PF₆
molecular formula	C ₆₀ H ₆₀ N ₄ O ₆ P ₄ F ₂₄	C ₇₃ H ₈₃ N ₁₃ O ₇ P ₄ F ₂₄	C ₇₆ H ₈₄ N ₁₀ O ₈ P ₄ F ₂₄	C ₈₀ H ₉₂ N ₁₀ O ₁₀ P ₄ F ₂₄
crystal description	red, rod-shaped triclinic	red, platelet triclinic	light red, block triclinic	red, platelet triclinic
unit cell parameters	<i>a</i> = 10.163(3) Å	<i>a</i> = 15.304(7) Å	<i>a</i> = 13.690(2) Å	<i>a</i> = 14.021(3) Å
	<i>b</i> = 12.669(4) Å	<i>b</i> = 15.316(7) Å	<i>b</i> = 13.848(2) Å	<i>b</i> = 14.121(3) Å
	<i>c</i> = 14.245(5) Å	<i>c</i> = 21.776(14) Å	<i>c</i> = 24.046(4) Å	<i>c</i> = 22.210(5) Å
	α = 99.963(4)°	α = 95.059(7)°	α = 84.815(2)°	α = 94.628(2)°
	β = 107.120(3)°	β = 106.489(7)°	β = 85.732(2)°	β = 93.400(2)°
unit cell parameters	γ = 112.522(3)°	γ = 116.953(5)°	γ = 67.626(2)°	γ = 93.554(3)°
	<i>V</i> = 1531.98 Å ³	<i>V</i> = 4219.95 Å ³	<i>V</i> = 4194.23 Å ³	<i>V</i> = 4365.5(17) Å ³
<i>R</i> -factor (%)	5.95	7.62	7.63	8.45
space group	<i>P</i> 1	<i>P</i> 1	<i>P</i> 1	<i>P</i> 1
<i>Z</i>	1	2	2	2
DNP/CBPQT ⁴⁺ [π···π] distance (Å) ^a	3.31	3.24	3.23	3.24
DNP/CBPQT ⁴⁺ interplanar angle (deg)	2.1	3.34	3.29	3.26
		1.6	0.2	1.2
[C–H···π] distance (Å)	2.57	2.4	0.4	1.0
		2.55	2.47	2.56
[C–H···O] distance (Å)	2.27	2.62	2.58	2.59
		2.37	2.40	2.38
		–	2.29	2.68

^a Defined as the distance between the average plane of the bipyridinium subunit and the centroid of the DNP ring's fused C–C bond.

six solvent (MeCN) molecules, some of which are disordered. Disorder is also present in some of the PF₆[−] counterions and, to a smaller extent, in the π-donor ring in **2c·4PF₆** (vide infra). Apparently, in all three [2]catenanes, the DNP/CBPQT⁴⁺ interaction is the dominant [π···π] one, since the CBPQT⁴⁺ ring encircles the DNP ring in preference to the triazole rings or butadiyne units. The stabilizing interactions noted in **[9a ⊂ CBPQT]·4PF₆** are only slightly perturbed in **1b·4PF₆** and **2b·4PF₆**, a situation which is most likely caused by the desymmetrization of the DNP/CBPQT⁴⁺ recognition motif and by the more constricted geometry of the cyclic π-donor.³⁷ Intriguingly, the newly incorporated 1,2,3-triazole (**1b·4PF₆**) and 1,3-butadiyne (**2b,c·4PF₆**) moieties align themselves with the outside face of one of the bipyridinium units of the CBPQT⁴⁺ ring, forming almost evenly spaced (outer)bipyridinium–DNP–(inner)bipyridinium–triazole/butadiyne layers.

In **1b·4PF₆** (Figure 4), the distance between the centroid of the triazole ring and the average plane of the inner bipyridinium unit is 3.38 Å, very close to that of the DNP–bipyridinium separation. Additionally, the two planes are nearly parallel (7.3°) with the triazole ring being slightly offset relative to one of the two pyridinium rings. Both of these effects can be interpreted as caused by the [π···π] stacking of the two units. The Cambridge Structural Database (CSD) reports three structures that include formally both the pyridinium ring and the 1,2,3-triazole unit, the former being incorporated into an *N*-pyridinium oxide unit, the latter into a benztriazole system.³⁸ In one of them,^{38a} intermolecular stacking between the triazole and

pyridinium rings resembles closely the case of **1b·4PF₆**, with an interplanar angle of 2.3° and a distance of 3.62 Å between the triazole centroid and the pyridinium plane. Alternating donor–acceptor stacks, observed in some of CBPQT⁴⁺-based catenanes,^{12a,39} are notably absent in the supramolecular stacks of **1b·4PF₆**. Instead, [2]catenane molecules pack around the crystallographic inversion center and are separated by two sandwiched and ordered PF₆[−] counterions and four MeCN molecules. The sandwiched PF₆[−] ions were completely refined and showed close F···H contacts to both the π-donor (glycolic chain CH₂, 2.47 Å) and π-acceptor (α-CBPQT⁴⁺, 2.35 Å) hydrogen atoms.

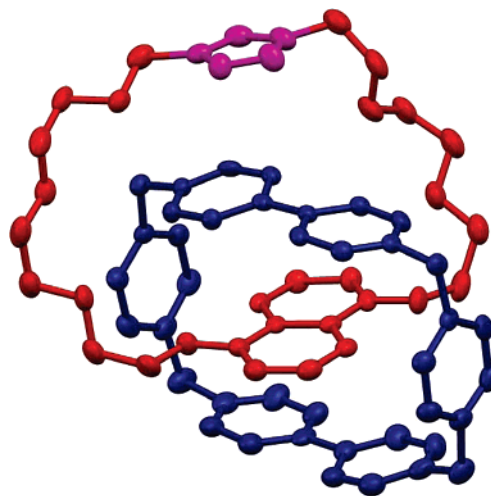


Figure 4. Solid-state structure of **1b⁺**. Aside from the disordered PF₆[−] counterions, hydrogen atoms and solvent molecules are omitted for clarity. Thermal ellipsoids are shown at 50% probability levels. Acceptor ring is shown in blue, donor thread in red, and triazole ring in purple.

Catenanes **2b,c·4PF₆** align their butadiyne fragments approximately parallel with the electron-poor inner bipyridinium unit, in sharp contrast to the nearly perpendicular orientation observed in DNP–phthalimide-based butadiyne-containing

(36) The ~45° tilt between the average planes of the π-donor and the π-acceptor rings in the catenanes **1b,c·4PF₆** and **2b,c·4PF₆** generates an element of helical chirality, such that molecules with (*P*) and (*M*) helicities can be identified. Additionally, 1,5-dioxynaphthalene and 1,2,3-triazole rings lose their symmetry elements once incorporated into a macrocycle. This desymmetrization imparts planar chirality of either a (*pR*) or a (*pS*) sense to both rings. Overall, these considerations mean that **1b,c·4PF₆** can exist as a total of 2³ = 8 diastereoisomers, while **2b,c·4PF₆** could exist as a total of four diastereoisomers. X-ray crystallography, and ¹H NMR spectroscopy reveal evidence for the existence of only one enantiomeric pair in the solid and solution states, respectively.

(37) One of the [C–H···O] interactions is notably lost in **1b·4PF₆** (Table 1) because of the geometry of the glycolic chain in the donor.

(38) (a) Katritzky, A. R.; Kurz, T.; Zhang, S.; Voronkov, M.; Steel, P. J. *Heterocycles* **2001**, 55, 1703–1710. (b) Savrda, J.; Ziane, N.; Guihne, J.; Wakselman, M. *J. Chem. Res.* **1991**, 2, 36–37.

(39) Ortholand, J.-Y.; Slawin, A. M. Z.; Spencer, N.; Stoddart, J. F.; Williams, D. J. *Angew. Chem., Int. Ed. Engl.* **1989**, 28, 1394–1395.

donor–acceptor catenanes reported by Sanders and co-workers.^{16a–b,27a,40} In **2b**·4PF₆ (Figure 5), the average distance between the plane of the inner bipyridinium unit and the atoms of the C≡C–C≡C axis is 3.50 (±0.07) Å. The bipyridinium N⁺–N⁺ vector is roughly coplanar with the C≡C–C≡C vector, with a torsional angle of 0.50°. Worthy of note is the virtually unstrained H₂C–C≡C–C≡C–CH₂ unit, with an overall deformation of a mere 9.8° spread over six atoms.⁴¹ Although the CSD does not report any structures with both the pyridinium and butadiyne fragments, analogous interactions between electron-poor arenes and butadiyne-containing systems are known. Hexafluorobenzene, for example, stacks efficiently with one of the butadiyne subunits of dehydrobenz[12]annulene⁴² with an average distance between the aromatic plane and the atoms of the C≡C–C≡C chain of 3.34 (±0.06) Å. As in the case of **1b**·4PF₆, no donor–acceptor stacks have been observed. Curiously, and unlike **1b**·4PF₆, the two molecules of **2b**·4PF₆ are not separated by counterions. Instead, C≡C–C≡C subunits are the closest point of contact, with a centroid–centroid distance of 4.98 Å and the closest contact between carbon atoms³⁵ being 3.73 Å.

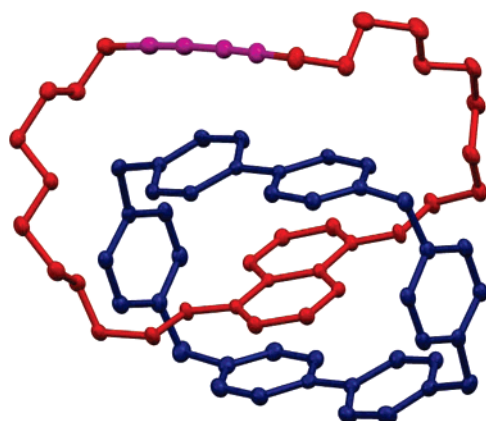


Figure 5. Solid-state structure of **2b**⁴⁺. Aside from the disordered PF₆[−] counterions, hydrogen atoms and solvent molecules are omitted for clarity. Thermal ellipsoids are shown at 50% probability levels. Acceptor ring is shown in blue, donor ring in red, and butadiyne moiety in purple.

The crystal structure (Figure 6) of the larger butadiyne-based [2]catenane **2c**·4PF₆ is analogous to that of **2b**·4PF₆, at least with regard to the alignment of the 1,3-butadiyne unit with the inner bipyridinium plane and despite the evident disorder in the diyne subunit and its immediate surroundings. Two equivalent conformations of the π -donor ring exist, and they are both in close contact with the bipyridinium unit, with average distances of 3.39 (±0.02) and 3.66 (±0.21) Å, respectively. Unlike in the case of **2b**·4PF₆, the bipyridinium N⁺–N⁺ vector is displaced at an angle of 26.8° (21.8° in the other conformation) with C≡C–C≡C vector. An overlay (Figure 7) of the

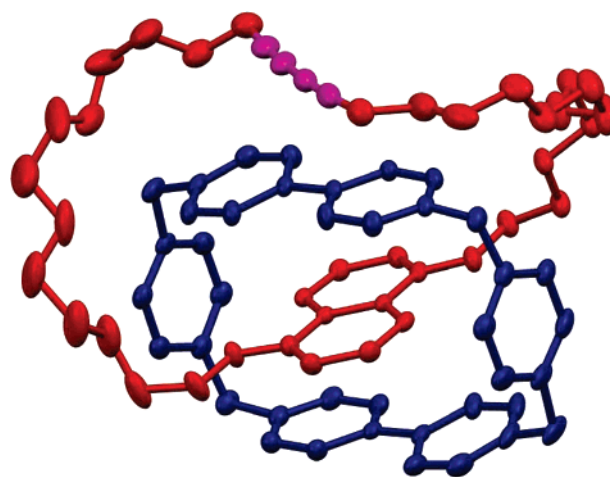


Figure 6. Solid-state structure of **2c**⁴⁺. Aside from the disordered PF₆[−] counterions, hydrogen atoms and solvent molecules are omitted for clarity. Thermal ellipsoids are shown at 50% probability levels. Acceptor ring is shown in blue, donor ring in red, and butadiyne moiety in purple. Only one of the two equivalent conformations of the diyne subunit is shown.

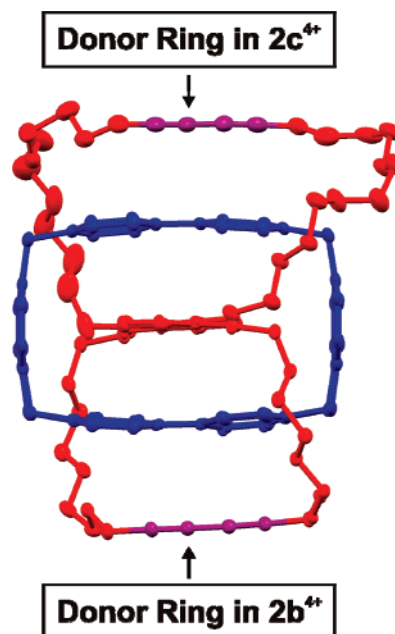


Figure 7. Comparison of the side views of the solid-state structures of **2b**⁴⁺ (bottom) and **2c**⁴⁺ (top). Structures were overlaid to maximize the overlap in their CBPQT⁴⁺ rings. Aside from the disordered PF₆[−] counterions, hydrogen atoms and solvent molecules were omitted for clarity. Flattening of the π -donating ring in **2c**⁴⁺ is evident (especially in the glycol chains) and necessary to bring the inner bipyridinium subunit of the π -acceptor into close contact with the butadiyne moiety of the π -donor.

structures of **2b**·4PF₆ and **2c**·4PF₆ shows visible flattening of the π -donor ring in the latter structure, acting to align the butadiyne and the bipyridinium units. Interestingly, the C≡C–C≡C units in **2c**·4PF₆ deform by 15.8 and 18.2° (depending on the conformation, overall over six atoms) to accommodate this close contact. These observations are a clear indication that the close butadiyne–bipyridinium contacts in **2b,c**·4PF₆ stem from a real interaction, rather than just a coincidental arrangement.

NMR Spectroscopic Studies

The importance of ¹H NMR spectroscopy in the characterization of donor–acceptor catenanes is manifold. Apart from the

- (40) (a) Hamilton, D. G.; Davies, J. E.; Prodi, L.; Sanders, J. K. M. *Chem.–Eur. J.* **1998**, *4*, 608–620. (b) Zhang, Q.; Hamilton, D. G.; Feeder, N.; Teat, S. J.; Goodman, J. M.; Sanders, J. K. M. *New J. Chem.* **1999**, *23*, 897–903.
- (41) Alkyne units have been known to deform readily in strained systems, in extreme cases up to 52° over the four atoms of the X–C≡C–X unit. See, inter alia: (a) Eisler, S.; McDonald, R.; Lopnow, G. R.; Tykewski, R. R. *J. Am. Chem. Soc.* **2000**, *122*, 6917–6928. (b) Gleiter, R.; Merger, R. In *Modern Acetylene Chemistry*; Stang, P. J., Diederich, F., Eds.; VCH: Weinheim, Germany, 1995; pp 285–319. (c) De Graaff, R. A. G.; Gorter, S.; Romers, C.; Wong, H. N. C.; Sondheimer, F. *J. Chem. Soc., Perkin Trans. 2* **1981**, 478–480. (d) Dosa, P. I.; Whitener, G. D.; Vollhardt, K. P. C.; Bond, A. D.; Teat, S. J. *Org. Lett.* **2002**, *4*, 2075–2078.
- (42) Bunz, U. H. F.; Enkelmann, V. *Chem.–Eur. J.* **1999**, *5*, 263–266.

confirmation of the constitutions of individual rings and the existence of mechanical interlocking, variable-temperature (VT) ^1H NMR spectroscopy probes the co-conformational dynamics within each of the rings. Installation of the 1,2,3-triazole ring or 1,3-butadiyne moiety into the skeleton of the donor macrocycle in catenanes is expected to affect the conformational and co-conformational flexibility of **1b,c**·4PF₆ and **2b,c**·4PF₆ as a result of the specific electronic and steric effects present in their component parts.

^1H NMR spectroscopy confirms the mechanically interlocked nature of all four compounds. The CBPQT⁴⁺ ring encircles the DNP unit exclusively, as reflected by the characteristically shielded DNP protons, giving rise to peaks at δ 6.29, 5.95, and 2.37 ppm (average values for all four of the [2]catenanes). See the Supporting Information for the individual values. The triazole protons in **1b,c**·4PF₆ resonate at δ 7.05 and 7.31 (CD₃-CN) ppm, respectively, as sharp singlets over a wide range of temperatures. These chemical shifts are notably different from the δ value of 8.60 ppm in a related [2]rotaxane,^{22a} suggesting shielding by the bipyridinium rings which lie in close proximity in the [2]catenanes. As a consequence of the absence of any protons associated with the butadiyne moiety in **2b,c**·4PF₆ and the inherent insensitivity of the ^{13}C NMR chemical shifts to ring current effects, NMR spectroscopy is not useful for probing the environments of the triple bonds within these catenanes.

Catenanes **2b,c**·4PF₆ contain the butadiyne unit which commutes with the C₂ axis of the DNP/CBPQT⁴⁺ assembly. In **1b,c**·4PF₆, this symmetry element is no longer retained on account of the unsymmetrical nature of the triazole ring.⁴³ With these symmetry considerations in mind, the ^1H NMR spectra of **1b,c**·4PF₆ and **2b,c**·4PF₆ are readily predicted. Assuming the completely “frozen” co-conformation shown in Figure 8, four

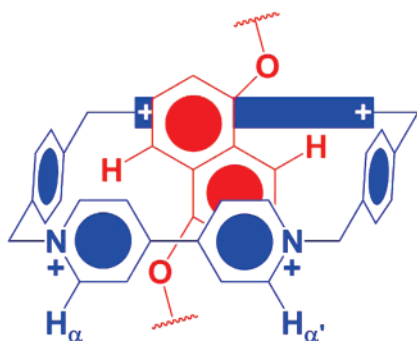


Figure 8. The DNP/CBPQT⁴⁺ assembly in donor–acceptor [2]catenanes. Hydrogen atoms relevant to the discussion are shown.

peaks would be expected for the α -CBPQT⁴⁺ ring protons in **2b,c**·4PF₆. One pair of peaks arises from the inequivalence between the inside and the outside α -CBPQT⁴⁺ protons, while the other pair is generated (Figure 8) by the heterotopicity of H _{α} and H _{α'} . The remaining four α -protons are related to the above-mentioned ones by the C₂ axis and thus appear to be equivalent. By contrast, in the triazole series, a total of eight different signals would be expected, since the C₂ axis is absent.

(43) The unsymmetric substitution of the triazole ring in **1b,c**·4PF₆ can potentially give rise to two diastereoisomers, depending on the orientation of the triazole relative to the pseudo-C₂ axis passing through the DNP and the CBPQT⁴⁺ rings. However, ^1H NMR spectra of both catenanes showed just a single set of CBPQT⁴⁺, DNP, and triazole peaks, consistent with the presence of only one (albeit unsymmetric) species.

Low-temperature ^1H NMR spectra agree well with these expectations based on symmetry arguments.

Although the conformational flexibility of the individual [2]-catenane components is encoded into the covalent structure of each ring, it is strongly influenced by the presence of a mechanically interlocking ring. On a higher hierarchical level—that of co-conformation—the interlocked structure itself is dynamic, as the two rings undergo a change in their geometrical relationship. The remainder of this section will be devoted to a discussion of conformational and co-conformational processes⁴⁴ (in that order) observed in **1b,c**·4PF₆ and **2b,c**·4PF₆.

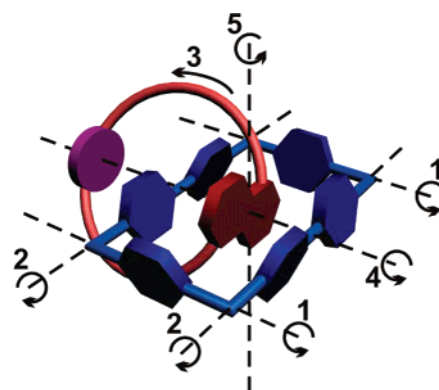
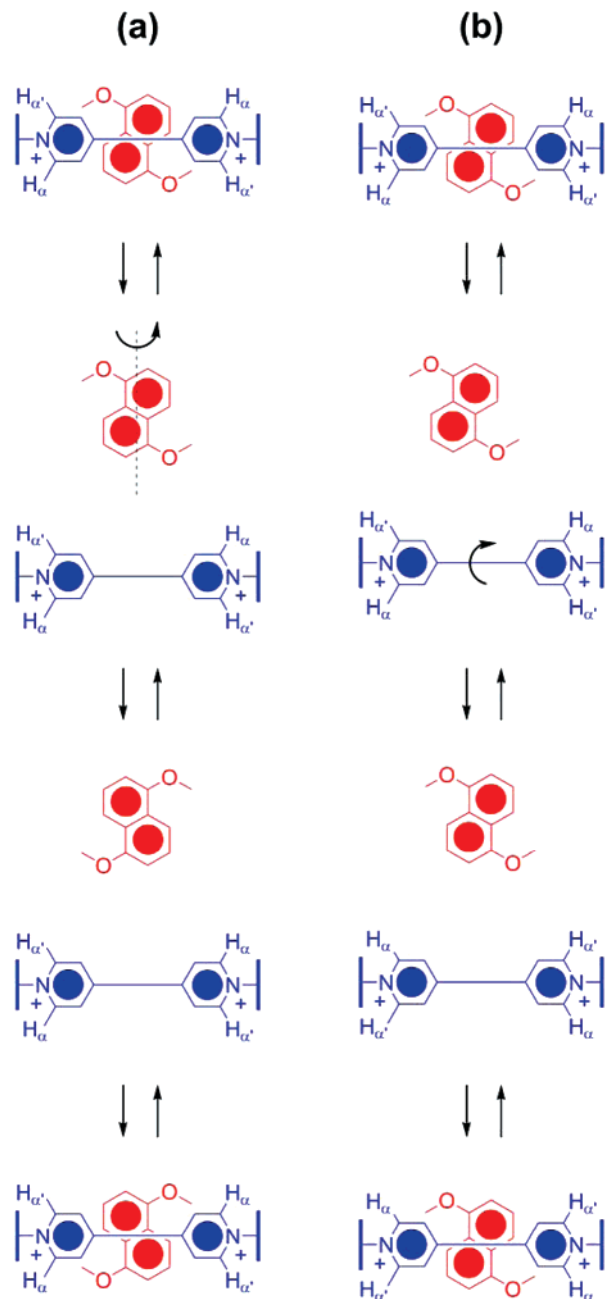


Figure 9. Conformationally and co-conformationally dynamic processes in the DNP-containing [2]catenanes can be interpreted as rotations around several different axes. The π -acceptor ring is shown in blue, the π -donor ring in red. Highlighted processes are: the phenylene rotation (axis 1), the bipyridinium rotation (axis 2), the circumrotation of the π -donor ring (process 3, also equivalent to the rotation of the donor ring around axis 2), ring rocking (incomplete rotation around axis 4), and the circumrotation of the π -acceptor ring (rotation of the acceptor ring around axis 5).

In the free CBPQT⁴⁺ ring, the rotations of both the phenylene and the bipyridinium units around their substitution axes (axes 1 and 2, respectively, in Figure 9) are fast on the ^1H NMR time scale. The situation changes in [2]catenanes where the unique combination of steric hindrance and intramolecular interactions slows down these conformational changes sufficiently to make them observable by ^1H NMR spectroscopy. The phenylene rotation (axis 1 in Figure 9) was followed by using the signals of the phenylene protons on the CBPQT⁴⁺ ring as probes. The completely conformationally (and co-conformationally) restricted representation of the CBPQT⁴⁺/DNP assembly shown in Figure 8 implies four sets of signals for **2b,c**·4PF₆ and eight for **1b,c**·4PF₆. The phenylene protons are influenced both by the phenylene rotation and the circumrotation of the CBPQT⁴⁺ ring (vide infra); if unrestricted, either of these two dynamic processes halves the number of observable signals. Ultimately, in the situation where all dynamic processes are uninhibited, the number of signals for the phenylene units in the ^1H NMR spectra of **1b,c**·4PF₆ and **2b,c**·4PF₆ reduces to one and two, respectively. The bipyridinium rotation (axis 2 in Figure 9) was followed by observing the signals corresponding to the H _{α} and H _{α'} atoms on the CBPQT⁴⁺ ring. Free bipyridinium rotation makes these two sets of hydrogen atoms symmetry related and thus equivalent—in turn decreasing the number of bipyridinium

(44) For a recent review of dynamics and stereochemistry of the CBPQT⁴⁺-based [2]catenanes, see: (a) Vignon, S. A.; Stoddart, J. F. *Collect. Czech. Chem. Commun.* **2005**, *70*, 1493–1576. See also: (b) Tseng, H.-R.; Vignon, S. A.; Celestre, P. C.; Stoddart, J. F.; White, A. J. P.; Williams, D. J. *Chem.–Eur. J.* **2003**, *9*, 543–556.

Scheme 4. Two Alternative Modes of Achieving the Formal Rotation of the Bipyridinium Moiety in the CBPQT⁴⁺-Containing [2]Catenanes



proton signals in half. However, steric considerations make the direct rotation of bipyridinium moieties impossible while the DNP unit is included inside the cavity of the CBPQT⁴⁺ ring. Two different mechanisms³³ which account for the apparent observation of bipyridinium rotation have been put forward. One possibility, summarized in Scheme 4a, is the displacement of the DNP ring from the CBPQT⁴⁺ cavity, followed by its 180° rotation around its O...O axis and its return into the binding pocket of the cyclophane. Otherwise (Scheme 4b), the DNP ring can leave the cyclophane binding site, temporarily allowing the free rotation of the bipyridinium rings in the CBPQT⁴⁺ ring before returning into the cyclophane cavity (in the original orientation). Since all the interactions that stabilize the DNP/CBPQT⁴⁺ ensemble need to be broken for either of these two mechanisms to act, a relatively high energy penalty can be

expected. The net effect of these two processes is the same, and they are indistinguishable by dynamic ¹H NMR spectroscopy.

In addition to conformational dynamics, Figure 9 shows three general aspects of co-conformational flexibility that have been previously observed⁴⁴ in CBPQT⁴⁺-based [2]catenanes. The first one is tantamount to the circumrotation of the π -donor macrocycle around the inside bipyridinium unit of the CBPQT⁴⁺ ring (rotation **3** in Figure 9). The second process is the partial rotation of the π -donor macrocycle around the axis of the mechanical bond between the two interlocked rings, in a motion reminiscent of rocking a cradle (rotation around axis **4** in Figure 9). Finally, in a third co-conformational change, the CBPQT⁴⁺ ring circumrotates⁴⁵ around the DNP unit of the π -donor macrocycle (otherwise viewed as the rotation around axis **5** in Figure 9). Fundamental limitations prevent the observation of the first two aforementioned processes. The circumrotation of the π -donor macrocycle (Scheme 5a) is unobservable⁴⁶ because of the nondegeneracy of the [2]catenanes reported in this investigation. The ring rocking is also nondegenerate as a result of the presence of [C–H... π] interactions in one co-conformation (Scheme 5b, left) and the absence of these contacts in the other co-conformation (Scheme 5b, right). The former co-conformation is the only species observed over a wide range of temperatures. Finally, the last co-conformational process—circumrotation of the CBPQT⁴⁺ ring around the DNP unit (Scheme 5a)—was monitored by following the signals of H _{α} and H _{α'} atoms (Figure 8) on the CBPQT⁴⁺ ring. Rotation around axis **5** maintains the inequivalence of these protons—since their chemical environments remain different at all times during the rotation—but equilibrates the “inside” and “outside” moieties of the CBPQT⁴⁺ ring and accordingly reduces the number of signals for α -bipyridinium protons in the spectra of **1b,c**·4PF₆ and **2b,c**·4PF₆ in half.

Dynamic ¹H NMR spectroscopy was performed in DMF-*d*₇ (bp 426 K, mp 212 K). The kinetic and thermodynamic parameters for the dynamic processes observed in **1b,c**·4PF₆ and **2b,c**·4PF₆ are summarized in Table 2. In some of the VT experiments, the predictions were obscured by (i) overlapping

(45) This process is sometimes referred to as the “pirouetting” of the π -donating ring around the formally motionless CBPQT⁴⁺ ring. We prefer to treat this motion from a different system of reference as the circumrotation of the π -accepting ring around the formally motionless π -donating ring. This semantic distinction emphasizes the geometric equivalence of the above process with the circumrotation of the π -donating ring (rotation **3** in Figure 9). In both processes, one of the rings formally rotates around the axis going through its center, while the other ring remains motionless (and vice versa). Hence, the difference in the spectroscopic consequences of the two processes comes from the difference in the *identity* of the rotating ring, and not from different *modes* of rotation. See ref 44a as well as: (a) Ashton, P. R.; Preece, J. A.; Stoddart, J. F.; Tolley, M. S.; White, A. J. P.; Williams, D. J. *Synthesis* **1994**, 1344–1352.

(46) The circumrotation of the π -donating ring around the inner bipyridinium unit of the π -accepting ring brings about equilibration between two co-conformations. In a degenerate system, these co-conformations are of equal energy and thus are equally populated at any given point. The barriers for circumrotation in such systems are easily derived from the corresponding coalescence parameters. In nondegenerate systems, such as **1b,c**·4PF₆ and **2b,c**·4PF₆, two co-conformations are not of equal energy; accordingly, their populations and the relative intensities of ¹H NMR signals are different. If the difference in population is sufficiently large (>95:5), the circumrotation will be fundamentally unobservable by NMR spectroscopy since the only observable species will be the more stable co-conformation. This situation is spectroscopically indistinguishable from an alternative in which circumrotation does not occur at all. Although highly unlikely, in light of our previous studies on related degenerate donor–acceptor [2]catenanes, the absence of π -donating ring circumrotation in **1b,c**·4PF₆ and **2b,c**·4PF₆ cannot be completely dismissed.

Table 2. Kinetic and Thermodynamic Parameters for the Dynamic Processes Observed in Catenanes **1b,c**·4PF₆ and **2b,c**·4PF₆

compd	1b ·4PF ₆	1c ·4PF ₆	2b ·4PF ₆	2c ·4PF ₆
Bipyridinium Rotation (Figure 9, axis 2)				
protons observed	—	—	α -CBPQT ⁴⁺	β -CBPQT ⁴⁺
$\Delta\nu$ (Hz)	—	—	98	28.5
k_c (s ^{−1})	—	—	217	63
T_c (K) ^a	—	—	362	288
ΔG_c^\ddagger (kcal mol ^{−1})	—	—	17.5	14.5
CBPQT ⁴⁺ Ring Circumrotation (Figure 9, axis 5)				
protons observed	α -CBPQT ⁴⁺	α -CBPQT ⁴⁺	α -CBPQT ⁴⁺	—
$\Delta\nu$ (Hz)	180	240	85 (60) ^b	—
k_c (s ^{−1})	400	533	190 (134) ^b	—
T_c (K) ^a	337	300	270	—
ΔG_c^\ddagger (kcal mol ^{−1})	15.8	13.8	13.1 (12.9) ^b	—

^a Calibrated using neat MeOH ($T < 295$ K) or ethylene glycol ($T > 295$ K) samples. ^b Two sets of α -CBPQT⁴⁺ protons gave slightly different values for the peak separation in the slow exchange limit.

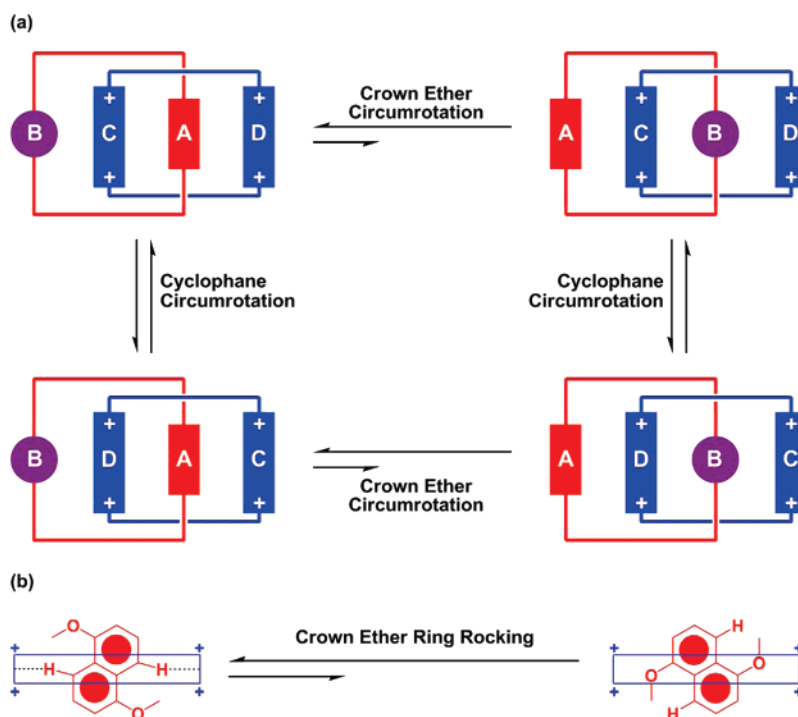
between the peaks, (ii) accidentally isochronous peaks, and (iii) the limited temperature range that could be explored experimentally.

The VT ¹H NMR spectra of **2b**·4PF₆ are the easiest ones (Figure 10) to analyze. The low-temperature (231 K) ¹H NMR spectrum of **2b**·4PF₆ features four doublets in the region associated with α -bipyridinium protons on the CBPQT⁴⁺ ring. With increasing temperature, these doublets start broadening and ultimately coalesce into two signals at 270 K, corresponding to a ΔG_c^\ddagger value of 13.0 kcal mol^{−1} for the circumrotation of the CBPQT⁴⁺ ring (axis **5** in Figure 9).⁴⁷ This value is ~ 1.0 kcal mol^{−1} higher than that observed³³ in previously studied DNP/CBPQT⁴⁺-containing [2]catenanes, possibly because of the smaller size of the π -donating ring in **2b**·4PF₆. A further increase in temperature causes the sharpening of these two peaks into well-resolved doublets (313 K). Finally, at 362 K, all signals corresponding to the α -bipyridinium protons on the CBPQT⁴⁺

ring collapse into a single peak which continues to sharpen beyond the coalescence point. A ΔG_c^\ddagger value of 17.5 kcal mol^{−1} was obtained for the bipyridinium rotation (axis **2** in Figure 9) in the CBPQT⁴⁺ ring of **2b**·4PF₆.

Although we were not able to obtain equally comprehensive data for the remaining three [2]catenanes, the information accumulated agrees with our expectations. In **2c**·4PF₆, the donor chain is longer, which is expected to allow some relaxation of the [2]catenane skeleton and accordingly lower the corresponding rotation barriers. Indeed, the bipyridinium rotation is facilitated by some 3 kcal mol^{−1}. The separation of peaks corresponding to the lower-energy process, the presumed halting of the circumrotation of the CBPQT⁴⁺ ring, could not be observed down to 231 K.

In the triazole series, **1b**·4PF₆, the smallest catenane prepared in this investigation, has an expectedly high barrier of 15.8 kcal mol^{−1} for the circumrotation of the CBPQT⁴⁺ ring. In its

Scheme 5. Co-conformational Processes in Donor–Acceptor [2]Catenanes (A = DNP, B = 1,2,3-Triazole or 1,3-Butadiyne, C = D = Bipyridinium)^a

^a (a) Circumrotation of the π -donating ring (horizontal arrows) and the π -accepting ring (vertical arrows). The unequal population of species with encircled DNP (A) and those with encircled 1,2,3-triazole/1,3-butadiyne (B) moieties renders the former process unobservable by ¹H NMR spectroscopy. (b) Ring-rocking of the π -donating ring, also unobservable as a result of unequal populations of the two states.

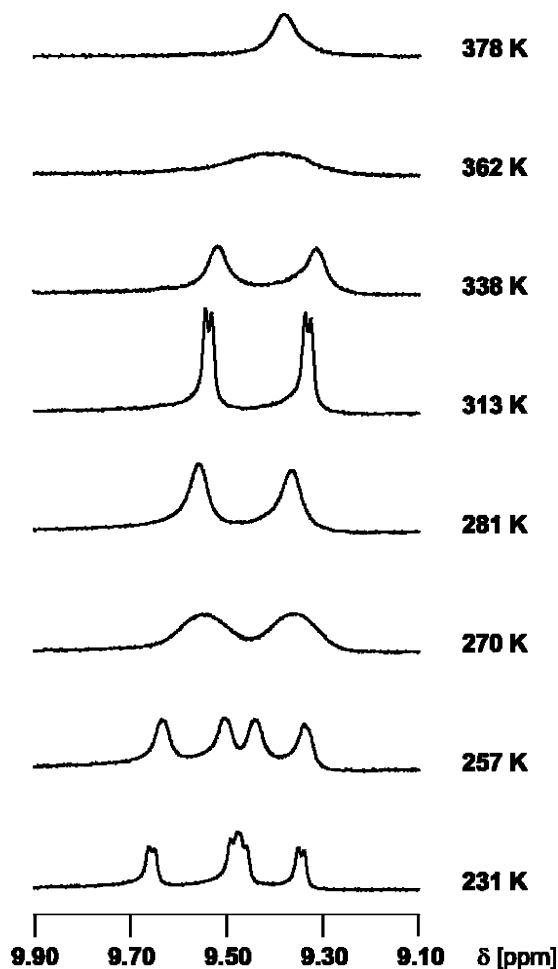


Figure 10. Partial VT ^1H NMR spectra of $2\text{b}\cdot 4\text{PF}_6$.

homologue, $1\text{c}\cdot 4\text{PF}_6$, this barrier is lowered to $13.8\text{ kcal mol}^{-1}$, consistent with the larger, more relaxed constitution of the π -donor. In $1\text{b},\text{c}\cdot 4\text{PF}_6$, we were unable to observe evidence of the bipyridinium rotation—i.e., further simplification of ^1H NMR spectra—on account of the extensive overlapping between the signals associated with CBPQT^{4+} protons. Differences in observed coalescence temperatures and the chemical composition of the four catenanes call for caution in making comparisons between the different systems. Nevertheless, two evident trends

emerge, namely (i) the higher rigidity of smaller catenanes as evidenced by the higher barriers and (ii) greater flexibility of butadiyne-containing catenanes relative to their triazole-containing counterparts. Evidence for the occurrence of this final dynamic process, that of phenylene rotation, was observed only in $2\text{c}\cdot 4\text{PF}_6$, allowing us to estimate a barrier of $14.4\text{ kcal mol}^{-1}$. In all of the other catenanes investigated, the peak overlap was too extensive to allow barriers to conformational and co-conformational change to be measured.

Conclusion and Outlook

The results presented in this paper demonstrate that [2]-pseudorotaxanes, constructed from chemically sensitive CBPQT^{4+} cyclophane and DNP-based π -donor components, and held together by noncovalent interactions, can act as synthons in a classical synthetic organic chemistry sense. Two tolerant reactions were employed as a proof of this concept, which appears to be broadly applicable. Extension of these protocols to other reactions is being pursued actively, with palladium-catalyzed cross-couplings being one of our primary target reactions. The Eglinton coupling emerges as a tolerant, simple, and efficient preparative method for making bipyridinium-based catenanes. This development, coupled with the rigid linear geometry and unique reactivity of butadiyne units, may open up new avenues of research based on this constitution. For example, higher ordering of catenanes could be achieved using butadiyne (and triazole) fragments as docks for transition metals.⁴⁸ The demonstrated utility of rigid molecular components in the construction of nanodevices⁴⁹ makes catenanes and rotaxanes with alkyne-based binding sites an appealing prospect.

Acknowledgment. This work was supported by the Microelectronics Advanced Research Corporation (MARCO) and its focus center on Functional Engineered NanoArchitectonics (FENA), and also by the Defense Advanced Research Projects Agency (DARPA) and the Center for Nanoscale Innovation for Defense (CNID). Dr. Ivan Aprahamian (UCLA) is acknowledged gratefully for insightful discussions.

Supporting Information Available: Experimental details, spectroscopic data for all new compounds, packing diagrams for $1\text{b}\cdot 4\text{PF}_6$, $2\text{b}\cdot 4\text{PF}_6$, $2\text{c}\cdot 4\text{PF}_6$, and $[9\text{a} \subset \text{CBPQT}]\cdot 4\text{PF}_6$ in the solid state, and VT-NMR spectroscopic data; crystallographic information files (CIFs) for $1\text{b}\cdot 4\text{PF}_6$, $2\text{b}\cdot 4\text{PF}_6$, $2\text{c}\cdot 4\text{PF}_6$, and $[9\text{a} \subset \text{CBPQT}]\cdot 4\text{PF}_6$; full refs 6j, 11c, 12c, 14, 15c, 30a, 33, 48b, 49a, and 49b. This material is available free of charge via the Internet at <http://pubs.acs.org>.

JA071319N

- (47) (a) Ōki, M. *Applications of Dynamic NMR Spectroscopy to Organic Chemistry*; VCH, Weinheim, 1985. (b) Gasparro, F. P.; Kolodny, N. H. *J. Chem. Educ.* **1977**, *54*, 258–261.
 (48) See, inter alia: (a) Hamilton, D. G.; Sanders, J. K. M. *Chem. Commun.* **1998**, 1749. (b) Ashton, P. R. et al. *Chem.–Eur. J.* **1998**, *4*, 590–607.
 (49) (a) Liu, Y. et al. *J. Am. Chem. Soc.* **2005**, *127*, 9745–9759. (b) Huang, T. J. et al. *Appl. Phys. Lett.* **2004**, *85*, 5391–5393.